Journal of Materials Chemistry C

Accepted Manuscript

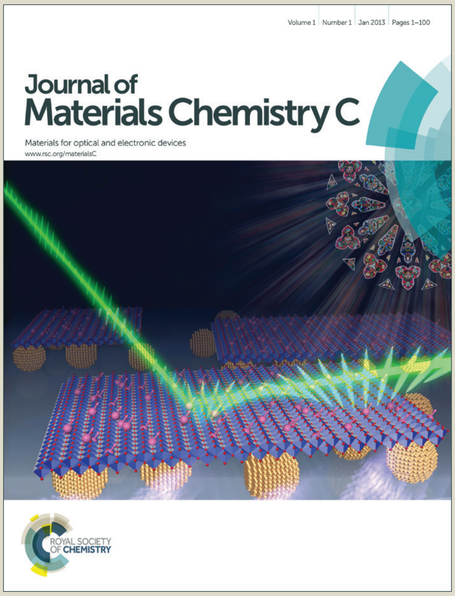

ROYAL SOCIETY OF CHEMISTRY

www.rsc.org/materialsC

Journal of Material Chemistry C RSCPublishing

COMMUNICATION

Cross-dipole stacking molecule of an anthracene derivative: integrating optical and electrical properties

Cite this: DOI: 10.1039/x0xx00000x

Received 00th January 2012,
Accepted 00th January 2012

DOI: 10.1039/x0xx00000x

www.rsc.org/

Jie Liu,[a,b] Lingqiang Meng,[b,c] Weigang Zhu,[a] Congcong Zhang,[d] Hantang Zhang,[a,b] Yifan Yao,[a,b] Zongrui Wang,[a,b] Ping He,[a, b] Xiaotao Zhang,[a] Ying Wang,[c] Yonggang Zhen,[a] Huanli Dong,[a] Yuanping Yi[a] and WenpingHu[a,d,*]

Cross-dipole stacking has been addressed as a preferred motif for solid state emission, but inefficient for charge transport. Here we synthesize a new anthracene derivative, which adopts cross-stacking in solid state with solid state fluorescence up to 77.3% and hole mobility of 1.47 cm^2/Vs, integrating optical and electrical properties successfully. As far as we know, it is the first report of organic field-effect transistors based on cross-dipole stacking molecules.

Relationships between molecular packing and chemical physical properties have been one of the most studied subjects in organic electronics.[1-3] Molecular packing modes can be generally classified into H-aggregation,[4] J-aggregation[5,6] and X-aggregation (cross-dipole stacking).[7-9] For H-aggregations, usually strong molecular π-π interactions are expected, which facilitate charge transport efficiently but inefficient for emission.[10] Comparing with H-aggregations, the dipole-dipole interactions in J-aggregations are relatively smaller, which might ensure emission property as well as part of charge transport properties.[6] X-aggregation, which has been studied both therotically and experimentally, is the most efficient in preventing luminescence queching in solid state.[7,11] For example, an distyrylbenzene derivative (*trans*-DPDSB) with a cross stacking structure was found with pure blue emission,[7] and an anthracene derivative of BDPVA was characterized with cross stacking and high flourescence too.[8] However, no reports on charge transport property of such molecules has been recorded because of the poor intermolecular overlap.

In order to integrating optical and electrical properties in one organic material simultaneously, we carry out this study and select anthracene derivatives as the candidates because anthracene itself is characterized with both optical and electrical properties.[12,13] Up to now, anthracene derivatives with high charge transfer properties are mainly based 2,6-substitution,[14-16] and highly florescent materials are addressed for 9,10-substituted anthracene derivatives.[17,18] We believe if bulky groups are introudced into the molecule skeleton, molecular distance of the π-conjugation could be enlarged, which might contibute to the minimization of the queching of emission in solid states just like in diluted solution or dispersed state in polymer matrix.

A new compound, 2,6-diphenylanthracene-9,10-diyl)bis (ethyne-2,1-diyl)bis(triethyl-silane) (TES-DPA) is synthesized, which is an anthracene derivative with enlarged π-conjugation along the long axis, and bulky substituion at the short axis. Single crystal analysis revealed that cross dipole stacking structure is adopting for TES-DPA. Moreover, fluorescence quantum yield (Φ_F) of 77.3% is determined for crystalline state of TES-DPA and mobility of 1.47 cm^2/Vs is obtained for its single crystal OFET devices.

The synthesis of TES-DPA is shown in Scheme 1. Starting from 2,6-diaminoanthracene-9,10-dione, Sandmeyer reaction,[19] Suzuki coupling reaction[20] are taken place successively to get 2,6-diphenylanthracene-9,10-dione, further addition of triethylsilylethynyllithium followed by deoxygenation with stannous chloride[21] give the target molecule with 46% yield.

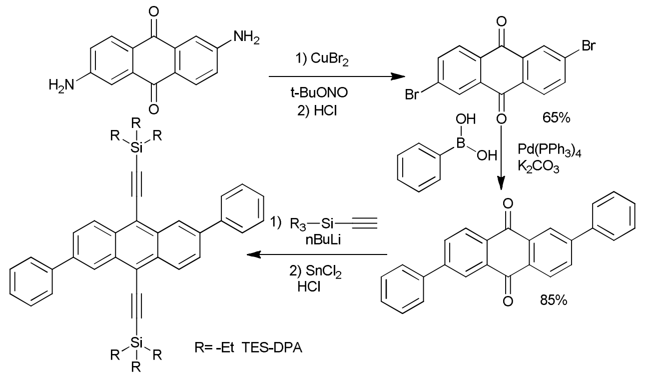

Scheme 1. Synthetic route of TES-DPA.

Single crystals of TES-DPA are grown by slow evopration from chlorobenzene solution. Crystal with a size of 0.24 mm × 0.12 mm × 0.10 mm is selected for single crystal analysis. As shown in Fig. 1A, isomers with different conformations coexist in the solid state (M1, M2, M3). Varied twisted angles is demonstrated for the substituted benzen rings of the three isomers. For M1, the two benzen rings are found with torsion angles of 28.46° and 43.07°, and the benzen rings in M2 and M3 show the same torsion, with torsion angles of 23.81° and 29.59°, respectively. The crystal belongs to $P\ 2_1/c$ space group with cell parameters of a = 26.848 (2) Å, b = 34.169 (2) Å, c = 7.6508 (6) Å and β = 90.500 (5)°. Packing modes of TES-DPA are shown in Fig. 1B, it can be observed that M2 stacks over M3 with a rotation angle of 60° and molecular distance of 7.007 Å for M2-M2 and 7.022 Å for M3-M3. M1 stacks over M1 with a rotation angle of about 60° and a distance of 7.079 Å for the nearest parallel pairs (Fig 1C). According to previous study, this packing mode might guarante high emission in solid state[7,8] and the residue π-π overlap between adjacent molecules along c-axis might made it possible for charge transport. Transfer integrals (based on single crystal data) along the cross-dipole stacking directions are calculated at the DFT-B3LYP/6-31G** level by using a fragment orbital approach in combination with a basis set orthogonalization procedure,[22] and t_h is determined as 137 meV for the M2-M3 stackings, and 126 meV for the M1-M stackings, which indicates that efficient hole transport might be expected along this direction.

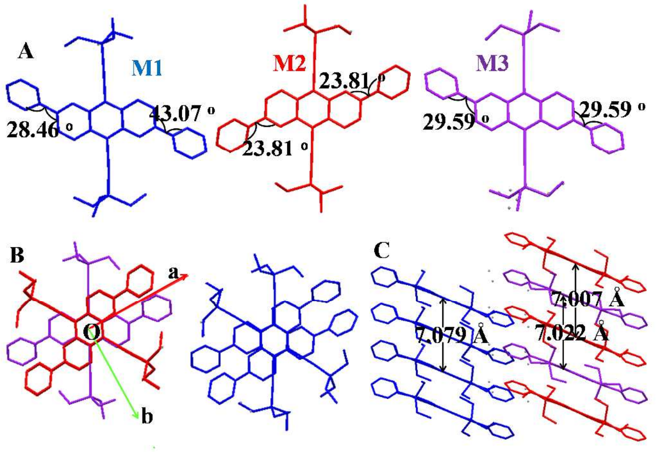

Fig. 1 A. Different conformational isomers in TES-DPA single crystal; B. packing modes of TES-DPA, and the molecules rotate about 60° along the stacking direction (c-axis); C. Molecular distances between adjacent parallel molecules.

To identify the stability of TES-DPA, a series of tests are conducted. Through thermal gravimetric analysis (TGA), decomposition temperature of 316 °C is found for TES-DPA (Fig. 2). Cyclic voltammetry (CV) measurements are performed under nitrogen with ferrocene as inner standard. The highest occupied molecular orbit (HOMO) and the lowest unoccupied molecular orbit (LUMO) are determined at -5.57 eV and -3.1 eV, respectively. The bandgap is calculated about 2.47 eV. By performing UV-*vis* absorption of TES-DPA, a bandgap of 2.63 eV is extracted from the onset absorption, which is well agreed with the results of CV. Corresponding emssion spectrum of TES-DPA in THF is shown in Fig. 2C with well structred vibrational peaks of typical anthracne derivatives. However, unlike *trans*-DPDSB and BDPVA, a much larger bathochromic-shift and vanished fine structres are observed for PL spectrum of TES-DPA single crystals (Fig. 2C), indicating different molecular interactions might be expected.[7,8] Moreover, Φ_F of 100% (Fig. S2) and 77.3% is determined for TES-DPA solution and crystalline solid, respectively.[23] Time resolved fluorescence spectrum of TES-DPA are shown in Fig. S3, fluorescence lifetime (τ_{FL}) of solid state (69.2 ns) is significantly increased as compared to that of solution (10.5 ns), and both fluorescence lifetimes accord well with the mono-exponential decay model, indicting the simple excited state for solution and crystals. Further calculation of radiative deactivation rate (k_r) reveals that k_r is decreased in crystals ($1.1\times10^7\ s^{-1}$) compared with that in soluitons ($9.5\times10^7\ s^{-1}$), which is quite different from BDPVA. Hence, although TES-DPA has similar packing structures as that of *trans*-DPDSB and BDPVA, but exhibits distinct photophyscial properties.[7,8] Further study on spectrometric behavior of TES-DPA is underway.

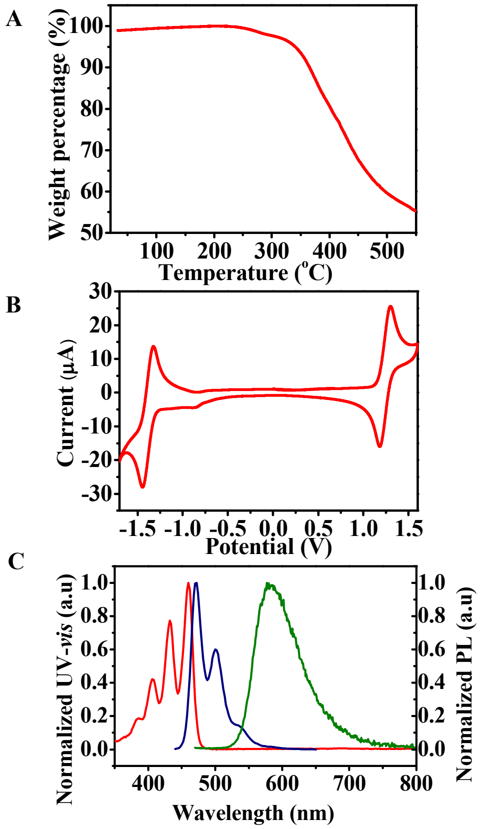

Fig. 2 A. TGA curve of TES-DPA; B. CV curve of TES-DPA in CH_2Cl_2 with concentration of 10^{-3} M; C. UV-Vis absorption (red) and florescent emission (blue) of TES-DPA in diluted solution with concentration of 10^{-5} M and photoluminescence of crystalline powder (green).

Crystals of TES-DPA can be easily grown by drop-casting. As shown in Fig. 3, crystals are obtained by using 0.05 mg/mL *n*-hexane solution of TES-DPA and they show high luminance under mercury lamp with an excitation wavelength of 380 nm. The cross-dipole stacking of the molecules along the c-axis induces one-dimensional growth of the micro- and nano-fibers and the molecular packing in these fibers is illustrated in Fig. 3 with M1, M2, M3 coexist in the cross section of the fibers.

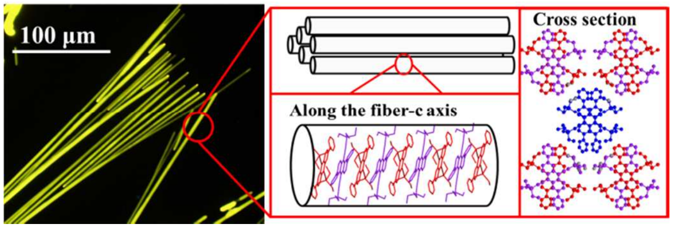

Fig. 3 Fluorescence microscope image of TES-DPA fibers and possible molecular packing.

Since efficient transfer integrals are obtained along the c-axis as mentioned above, it is worth testing the charge transport properties of TES-DPA. Single crystal devices based on micro- and nanofibers are fabricated on SiO_2/Si wafers with gold as source and drain electrodes. Typical transfer and output curves are shown in Fig. 4. The devices achieve a maximum mobility of 1.47 cm^2/Vs with a threshold voltage of about -4V and I_{on}/I_{off} of 10^4~10^5. As far as we know, this is the first report of OFET based on cross-dipole stacking molecules.

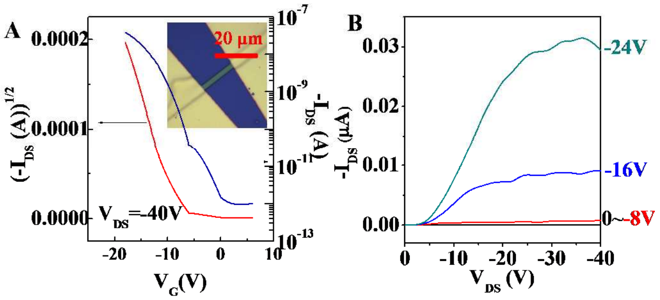

Fig. 4 A. Transfer curve of typical single crystal device base on TES-DPA, inset: an optical image of the device; B. corresponding output curves of the same device.

Considering the high emission of TES-DPA, it renders us its application in organic light-emitting diodes (OLEDs). As mentioned above, the HOMO and LUMO levels of TES-DPA are well aligned with the work function of PEDOT:PSS (5.1~5.2 eV) and LiF/Al (2.9~3.4 eV), which means that no additional layer is needed for charge injection in OLEDs of TES-DPA. As illustrated in Fig.5, the emission layer (EML) of TES-DPA (110 nm) is inserted directly between ITO/PEDOT:PSS anode and LiF/Al cathode. The energy-level diagram of the devices is shown in Fig. 5A. Indeed, nice yellow emission is observed from the OLEDs as the spectra shown in Fig. 5B and correponding J-V and L-V cures show in Fig. 5C and 5D, respectively. The turn on voltage of the devices is as low as 3.0 V indicating the efficient charge injection due to the well energy alignment. The maximum brightness is up to 3881 cd/m^2 (typical efficiency curves see Supplementary Information). It is understandable that the devices performance could be further optimized, and the optimization will be influnenced by the crystallinity of the material.

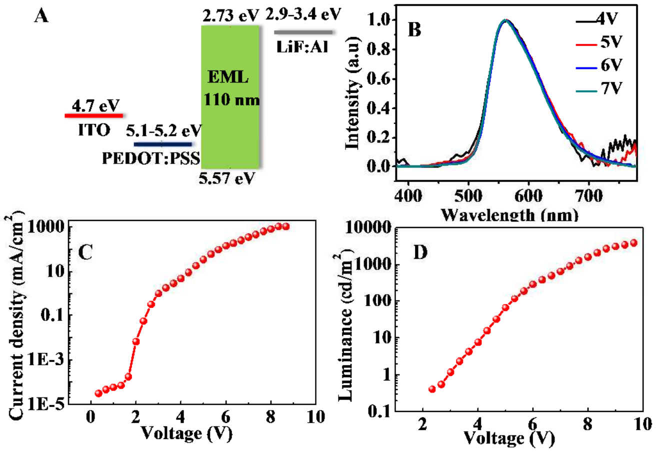

Fig. 5 A. Energy levels of the device; B. Eelectroluminance spectra of the devices; C- D. J-V and L-V curves of the devices.

In summery, by introducing the phenyl groups to 2,6-position and the bulky triethylsiylacetylene groups to 9,10-position of anthracene, a new compound TES-DPA is obtained. Single crystal analysis reveals that a cross-dipole stacking structure is achieved in its solid state. Moreover, single crystals of TES-DPA is determined with hole mobility up to 1.47 cm^2/Vs and Φ_F of 77.3%. Single layer OLEDs of TES-DPA show brigtness of 3881 cd/m^2 with turn on voltage of 3.0 V. As far as we know, it is the first report to integrate optical and electrical properties on one organic semiconductor, indicating its great potential in orgainc electronics.

Acknowledgements

The authors acknowledge National Natural Science Foundation of China (51222306, 91222203, 91233205, 91433115), the China-Denmark Co-project (60911130231), TRR61 (NSFC-DFG Transregio Project), the Ministry of Science and Technology of China (2011CB808405, 2011CB932304, 2013CB933403, 2013CB933504), the Strategic Priority Research Program of the Chinese Academy of Sciences (XDB12030300), Beijing NOVA Programme (Z131101000413038), and Beijing Local College Innovation Team Improve Plan (IDHT20140512).

Notes

[a] *Beijing National Laboratory for Molecular Science, Key Laboratory of Organic Solids, Institute of Chemistry, Chinese Academy of Sciences, Beijing 100190, China.*
[b] *University of the Chinese Academy of Sciences, Beijing 100190, China.*
[c] *Key Laboratory of Photochemical Conversion and Optoelectronic Materials, Technical Institute of Physics and Chemistry, Chinese Academy of Sciences, Beijing, 100190, People's Republic of China.*
[d] *Collaborative Innovation Center of Chemical Science and Engineering (Tianjin) & School of Science, Tianjin University, Tianjin 300072, China.*

† Electronic supplementary information (ESI) available: Experiments, synthesis procedures, crystallographic information, time-resolved fluorescence, current and power efficiency curves of the OLED device. For ESI and crystallographic data in CIF or other electronic format see DOI: 10.1039/c000000x/

References

1. R. J. Li, W. P. Hu, Y. Q. Liu and D. B. Zhu, *Acc. Chem. Res.*, 2010, **43**, 529-540.
2. M. Mas-Torrent and C. Rovira, *Chem. Rev.*, 2011, **111**, 4833-4856.
3. Y. N. Hong, J. W. Y. Lam and B. Z. Tang, *Chem. Soc. Rev.*, 2011, **40**, 5361-5388.
4. S.-O. Kim, T. K. An, J. Chen, I. Kang, S. H. Kang, D. S. Chung, C. E. Park, Y.-H.Kim and S.-K. Kwon, *Adv. Funct. Mater.*, 2011, **21**, 1616-1623.
5. S. Choi, J. Bouffard and Y. Kim, *Chem. Sci.*, 2014, **5**, 751-755.
6. Z. Xie, B. Yang, L. Liu and Y. Ma, *J. Mol. Eng. Mater.*, 2013, **01**, 1340002.
7. Z. Q. Xie, B. Yang, F. Li, G. Cheng, L. L. Liu, G. D. Yang, H. Xu, L. Ye, M. Hanif, S. Y. Liu, D. G. Ma and Y. G. Ma, *J. Am. Chem. Soc.*, 2005, **127**, 14152-14153.
8. J. Zhang, B. Xu, J. Chen, S. Ma, Y. Dong, L. Wang, B. Li, L. Ye and W. Tian, *Adv. Mater.*, 2014, **26**, 739-745.
9. N. Sanyal and P. M. Lahti, *Cryst. Growth. Des.*, 2006, **6**, 1253-1255.
10. S. A. Jenekhe and J. A. Osaheni, *Science*, 1994, **265**, 765-768.
11. J. Cornil, D. A. dos Santos, X. Crispin, R. Silbey and J. L. Brédas, *J. Am. Chem. Soc.*, 1998, **120**, 1289-1299.
12. A. N. Aleshin, J. Y. Lee, S. W. Chu, J. S. Kim and Y. W. Park, *Appl. Phys. Lett.*, 2004, **84**, 5383-5385.
13. M. Pope, P. Magnante and H. P. Kallmann, *J. Chem. Phys.*, 1963, **38**, 2042-2043.
14. J. E. Anthony, *Chem. Rev.*, 2006, **106**, 5028-5048.

15. M.-C. Um, J. Jang, J. Kang, J.-P.Hong, D. Y. Yoon, S. H. Lee, J.-J. Kim and J.-I. Hong, *J. Mater. Chem.*, 2008, **18**, 2234-2239.
16 L. Jiang, W. Hu, Z. Wei, W. Xu and H. Meng, *Adv. Mater.*, 2009, **21**, 3649-3653.
17. J. M. Shi and C. W. Tang, *Appl. Phys. Lett.*, 2002, **80**, 3201-3203.
18. J. T. He, B. Xu, F. P. Chen, H. J. Xia, K. P. Li, L. Ye and W. J. Tian, *J. Phys. Chem. C*, 2009, **113**, 9892-9899.
19. F. Bures, W. B. Schweizer, C. Boudon, J. P. Gisselbrecht, M. Gross and F. Diederich, *Eur. J. Org. Chem.*, 2008, 994-1004.
20. J. Liu, Q. Meng, X. Zhang, X. Lu, P. He, L. Jiang, H. Dong and W. Hu, *Chem.Commun.*, 2013, **49**, 1199-1201.
21. J. E. Anthony, J. S. Brooks, D. L. Eaton and S. R. Parkin, *J. Am. Chem. Soc.*, 2001, **123**, 9482-9483.
22. E. F. Valeev, V. Coropceanu, D. A. da Silva Filho, S. Salman and J. L. Brédas, *J. Am. Chem. Soc.*, 2006, **128**, 9882–9886.
23. X. Cao, S. Bai, Y. Wu, Q. Liao, Q. Shi, H. Fu and J. Yao, *Chem. Commun.*, 2012, **48**, 6402-6404.

Table of Contents:

Cross dipole stacking molecule: optical and electrical study

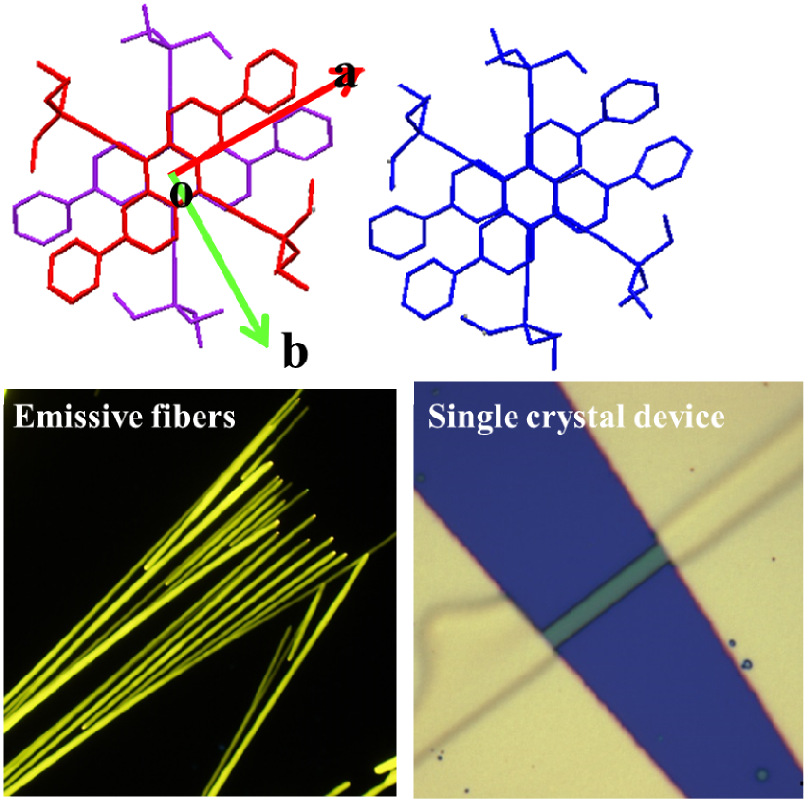

The present work showed the synthesis of a cross stacking molecule. And both semiconducting property and solid state luminescence were achieved for its micro/nano fibers.